American Journal of ORTHODONTICS

Founded in 1915 Volume 82, Number 3 **September 1982**

ORIGINAL ARTICLES

Dr. Bookstein

On the cephalometrics of skeletal change

Fred L. Bookstein
Ann Arbor, Mich.

This essay introduces the general tensor analysis of skeletal change for landmark data. Consider first a single triangle of landmarks at two times. Joint changes in the lengths of its sides, or in the positions of its vertices according to some coordinate system, may be taken to specify a uniform deformation of the entire interior. The biorthogonal method expresses this by a pair of *principal dilatations*—maximum and minimum rates of change in length—along directions lying at 90 degrees in some orientation upon the triangle. No analysis of static form is involved in their calculation, which measures shape change without measuring shape. From this basic biorthogonal decomposition, we pass by a suitable averaging to descriptions of mean change in groups of diverse initial form and subsequently to explicit comparison of two mean changes, such as "treatment effect," all in the same parameters: two dilatations and an orientation. Schemes of more than three landmarks may be analyzed by reduction to triangles. I exemplify the method using data from Sheldon Baumrind's study of Angle Class II treatment effects. With respect to the growth observed in a "control" group of untreated Class II cases, both "cervical" (headgear) and "intraoral" (activator) appliances have the effect of compressing a facial polygon horizontally (parallel to S-N) by about 1 percent per year and extending it vertically (perpendicular to S-N) by about 1 percent per year. These effects are slightly larger for the cervical treatment, which also causes an increase in the distance from nasion to the line sella-ANS (that is, "rotates the face downward") by some 1 percent per year relative to the growth observed in the controls.

Key words: Biorthogonal analysis, orthodontic treatment effects, shape change, cephalometrics, craniofacial growth, Cartesian transformations

This essay introduces the general tensor analysis of skeletal change for landmark data. The method results in diagrams such as those shown in Figs. 28 through 32, which deal with differences among orthodontic treatments for Angle Class II malocclusion. This article is intended to explain in full detail the explicit content of these diagrams, their meaning, and their geometric computation.

The essay is in seven parts: six text sections and an Appendix. Section I briefly characterizes the data bases for which the biorthogonal method is suited: triangulations and digitizations of anatomic landmarks. Section II explains the fundamental geometric manipulation resulting in the growth tensor for a single triangle of landmarks at two times; the Appendix presents a scheme for hand computation using only ruler and protractor. Section III suggests some modes of interpretation for the diagrams that result. Section IV shows how to average changes in populations of varying initial shape and how to compare two such averages. Section V, using some data collected by Baumrind and colleagues, exemplifies the analysis in a simple descrip-

From the Center for Human Growth and Development and the Department of Radiology, The University of Michigan.

0002-9416/82/090177+22$02.20/0

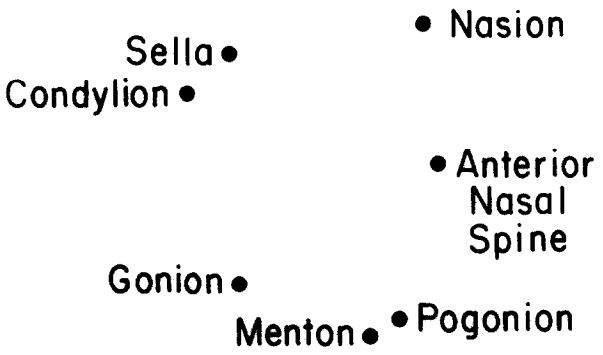

Fig. 1. Abstraction of the cephalogram: a configuration of isolated points, each characterized anatomically.

tion of treatment effects upon craniofacial growth. A last brief section comments upon certain limits of the method.

I. BASIC CEPHALOMETRIC DATA

Cephalometric data are of two general types: information about points and information about curves.[6] I shall assume here that only point data are available, so that every cephalogram is abstracted as a configuration of N isolated points, each of which has a name, as in Fig. 1. Points of the same name in different forms are taken to be anatomic homologues. This criterion excludes many conventionally acceptable landmarks: those whose definition is dependent on the preassignment of a fixed orientation, such as A, or the constraint of tangents at a distance, like orbitale, and those which are not properly pictures of points at all, such as articulare or "PtM." Generally, acceptable landmarks are those at which three structures meet (for instance, bregma and lambda) or which are intersections of sutures or other edges with the midsagittal symmetry plane (for instance, basion).

The scientist or clinician versed in cephalometrics is used to "measuring" the shape of these configurations by means of various distances, angles, and ratios. From such analyses we need no more nor less than an *archive*, sufficient information to permit the forms' complete reconstruction. This can always be managed with distance measures alone, by triangulation or digitization.

Triangulation

The N points may be reconstructed as a rigid body from 2N-3 interpoint distances measured in a particular pattern: a single distance measured between two landmarks L_1, L_2; then, two distances measured from each of the remaining (N-2) landmarks L_j, $j = 3, \ldots, N$, to any two of the points $L_1 \ldots L_{j-1}$ triangulated earlier. In this way the entire configuration is reassembled, vertex by vertex. Diverse schemes for a set of N = 7 landmarks are sketched in Fig. 2. Such collections of distance measures are not much suited to the purposes of multivariate morphometrics, the geometry-free study of the distances jointly via such techniques as factor analysis. To the extent that our purpose is the archiving of form, with considerations of measurement postponed until we are actually confronting explicit shape changes, we may ignore the infelicities of these distance networks as "variables"—they are adequate for storage of data.

Digitization

We can reconstruct the N landmark positions just as well from the list of their distances measured perpendicularly to two fixed lines at 90 degrees (Fig. 3). These quantities are likewise not of much use as statistical variables, since the straight lines with respect to which they are measured have no biologic reality. The number of distances supplied is two per point, totalling 2N; but three of these are arbitrary, comprising information about the coordinate axes themselves, their positions and orientation. We would be better served by the 2N distance coordinates of the N landmarks together with the two points anchoring the coordinate system, were it not for the accident that electronic digitizers supply the information we seek automatically. In any case, digitizations are much less convenient than triangulations for analysis and forecasting.

II. DESCRIPTION OF SHAPE CHANGE AS DEFORMATION

I shall assume that the cephalogram has been archived in one of these two forms, rather than by way of variables prescribed in some conventional analysis. What began as play of shadows on film is now a roster of some 2N distances measured between points or between points and lines. There is no explicit information about angles, proportions, intersections of straight lines, circles, or any other complex construct.

Our purpose is solely the measurement of change. One might hope that the quantities of the archive would serve to make this procedure a conceptual triviality; since these distances quantify forms separately, we have but to execute a few subtractions to produce the change scores. In attempt after attempt, this straightforward approach has proven a total failure, whatever algebraic mode is used. The distance parameters of the archive, and the quantities algebraically derived from them, cannot be held to usefully measure change of configurations, even though they exhaustively describe them; by

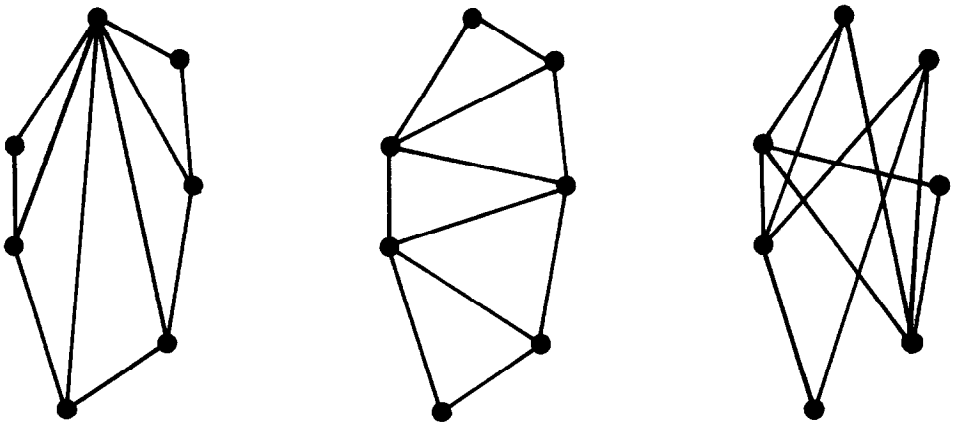

Fig. 2. Three triangulations for seven landmarks. The configuration may be reconstructed completely from many different sets of eleven measured distances, which are thus all equivalently informative.

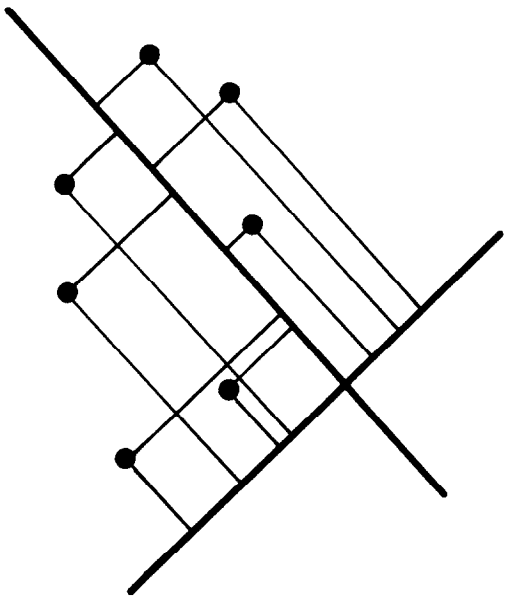

Fig. 3. Cartesian coordinates represent a configuration of points by distances from the points to two fixed lines at 90 degrees.

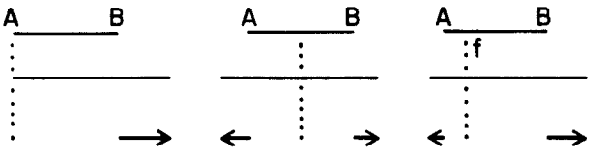

Fig. 4. Three "growth analyses" of a pair of landmarks observed at two times. There is no way to allocate observed growth between the landmarks.

and large, differences between coordinates or corresponding distances or other quantities for a pair of forms do not represent biologically interpretable aspects of the global contrast between them.

Quantifications of change relate to quantifications of form much more subtly than is generally imagined. The proper mode of measurement for shape change was first set out more than 60 years ago by the British natural philosopher D'Arcy W. Thompson in his classic *On Growth and Form*. He introduced the construction of shape change as a geometric operator, a deformation which maps one configuration onto another in accord with biologic homologies. The measurement of shape change ought to be the description of this operator directly, without particular reference to quantifications of the separate forms being compared.

As a tool for the description of deformation, Thompson offered his celebrated method of Cartesian transformation grids, which proved, however, resistant to quantification. Some years ago I suggested an alternative, the method of biorthogonal grids.[5] In this essay I reduce the method to its essentials so as to generalize its application from one comparison to many.

Let us explore possible measures of change for the simplest possible configuration, that of two landmarks only. The pair of configurations comprises two segments, as shown in Fig. 4. There is no information available about position or orientation of the segments; that would imply the presence of additional points in the configuration, which we do not have, to fix a coordinate system.

Cephalometricians are used to superimposing images at one point or another. For instance, one might superimpose at landmark A (Fig. 4, A); then point B appears to move to the right by a certain distance, dx. Or one might superpose at end B; then point A appears to move leftward by the same dx. We could equally

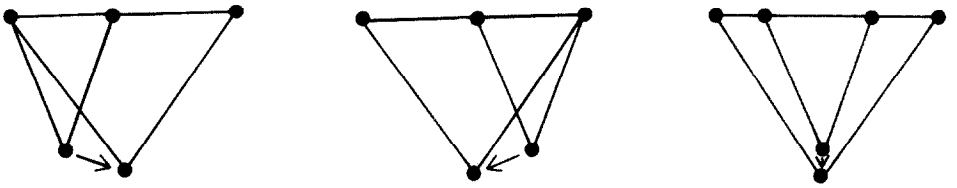

Fig. 5. Three "growth analyses" of a single triangle. By various superpositions on one edge, we may make the opposite vertex appear to be moving "forward," "backward," or neither.

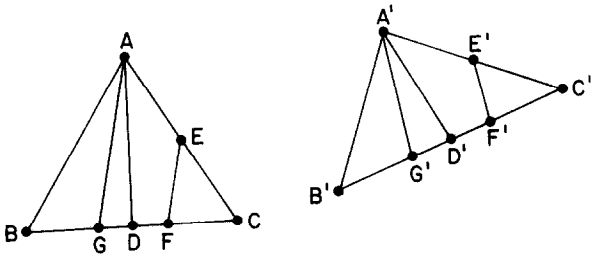

Fig. 6. Figure for the argument inferring homogeneity of deformation in an arbitrary direction. (See text.)

well superpose upon the centroids of the segments, as in Fig. 4, *B*; then *A* and *B* move away from the point of superposition by dx/2, one to the left and one to the right. In fact, for any fraction *f* between 0 and 1, superposition of the segments upon a point the fraction *f* of the way from *A* to *B* (Fig. 4, *C*) will result in an apparent displacement of *A* leftward by a fraction *f* of dx and a displacement of *B* rightward by the remainder, and any superposition whatever of the segments corresponds to this construction for some value of f inside or outside the proper interval. Subject to the discipline of data so minimal, all of the superpositions are equally plausible. We cannot unambiguously describe the relation of the segments in terms of changes at the end points separately.

This arbitrariness is intolerable; we must find a universal, unambiguous descriptor of the relation between the segments, a quantity identical from frame to frame of Fig. 4. For this simple situation, of course, we intuitively know the answer. The whole segment and all of its fragments increase their lengths by the same ratio, regardless of where we locate the "center" and how we measure "motion." The abstraction presumes only that the change is homogeneous between landmarks—a postulate the contravention of which requires more data than we are presuming here.

A distance ratio of this sort, taken from end to end of homologous segments between forms, is called a *dilatation*. If it is greater than 1.0, it represents a stretch or extension; if less than 1.0, a shrinking or compression. As the quotient of two quantities in the same unit of length, it is itself dimensionless.

For segments, the notion of dilatation is trivial. To arrive at a practical analysis of cephalograms, we must generalize its power from sets of two landmarks to sets of three, from pairs of segments to pairs of triangles. It is not immediately obvious how to proceed, since the three sides of the triangle are growing at three different rates.

One analogue of the two-point analysis is the construction of various superpositions in search of some common thread. As for segments, we quickly discover that no quantifications via displacements (now two-dimensional vectors) can be made unambiguous. For instance, it is common to speak of a point as "moving downward" or "moving forward" with respect to the segment formed from two other points, but by suitable choice of a center of superposition along that edge we can make the point in question appear to shift its sense of motion from "forward" to "backward" or to remain still. In a system generally increasing in size, all landmarks appear to be growing more or less radially away from any center of superposition placed homologously in the forms. Such "observations" are pure geometric artifacts which badly confound conventional quantitative comparisons (Fig. 5).

As for segments, it is fruitless to proceed with calculations that are so arbitrary. Rather than attempting to construct indices from the behavior of the separate parts of this figure, its points and edges, we need to adapt the stance of the two-point analysis and explicitly search for the universal descriptor, the one that is not a function of superposition.

Because we are working on a flat picture plane, that is, in Euclidean geometry, such a descriptor is available. Any data of the form we specified (two triangles of three landmarks) are consistent with a model of dilatations varying by direction only, and in a very simple way. To see why this should be so, let us attend to one of the landmarks, perhaps point *A*, and draw a line connecting it to some point *D* on the opposite edge, perhaps halfway from *B* toward *C*, as in Fig. 6. We have no information about this line beyond what we know of points *A*, *B*, and *C* in the two images. The one relevant "fact" is the assumption of homogeneity of

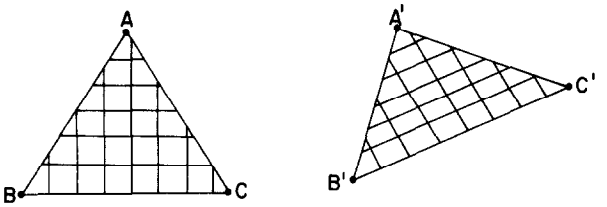

Fig. 7. Homogeneous Cartesian grid for the same transformation, in the style of D'Arcy Thompson.

transformation along side BC, treated as a segment all by itself; hence to point D corresponds a homologue D' halfway between B' and C' in the second image. In the absence of further information, such as might be supplied by a fourth landmark interior to the triangle, we must assume that the change along AD is to be described just like change along any other segment defined consistently with homology; that is, it is to be described by a single homogeneous dilatation.

Now, for any other segment transecting the triangle, such as EF, we may construct the line AG parallel to it. By linearity of homology on the side AB to E corresponds a proportional homologue E' in the second triangle. Likewise, F and G have proportional homologues F' and G', and the line $E'F'$ is parallel to the line $A'G'$. By a theorem from high-school geometry, the ratio of distances $E'F'/EF$ is the same as the ratio $A'G'/AG$. (It is in this step that the presumption of flatness takes effect, surreptitiously.) Then the dilatation along all lines parallel to AG is the same, so that dilatation is not a function of position.

In D'Arcy Thompson's grid system this homogeneity corresponds to an engridment the lines of which, although oblique, remain parallel and equally spaced within families (Fig. 7). I prefer to emphasize instead the measured parameter itself, the dilatation, whose homogeneity follows directly from the two-point analysis preceding. The two descriptions are quite equivalent.

By restricting our attention to only the data we are given—the three points in each of two images, with no auxiliary biologic information to engender inhomogeneities—we have reduced our model of shape change for the triangle to a system of dilatations varying by direction. Even though position within the triangle is no longer a consideration, however, it is still not obvious how we might "measure," that is, parameterize, dilatation as a function of direction.

The appropriate simplification results from diagramming the quantity of interest explicitly. Let us take the specimen deformation from Fig. 7 and draw out the dilatation function. We can, of course, do so implicitly, (Fig. 8, *A*); here the dilatation is to be read as the ratio

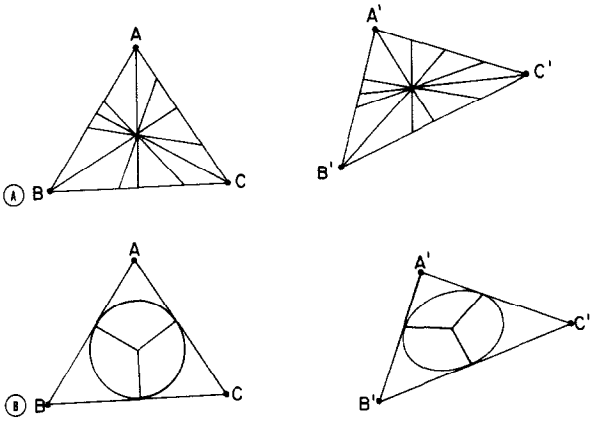

Fig. 8. The strain ellipse. **A,** Implicit display of dilatations as ratios of corresponding lengths. **B,** Explicit realization of dilatations as radii of the ellipse into which the deformation takes a circle.

of lengths for corresponding segments out of the centers. (Remember that "corresponding" is here defined by the cutting of equal fractions on the homologous sides, in accordance with the postulate of homogeneity there.) This is just a graphic version of the definition, in which the information we seek comes from a relationship between the two forms. To concentrate it in a single diagram, we execute the division graphically, by dilatating segments of constant length. The ratio we seek is then the actual length of the appropriate transformed segment and may be read in a single figure. Cutting the left-hand fan of Fig. 8, *A* by a circle, and adjusting the lengths of the segments on the right appropriately, we arrive at the display in Fig. 8, *B*, whose simplicity is astonishing and gratifying. When the left-hand segments are radii of equal length, the right-hand envelope looks remarkably like a perfect mathematical ellipse, and, as a matter of theorems algebraic or geometric, whose ancient proofs will be omitted here, that is precisely what it is.

For the homogeneous deformation, the dilatation function we seek is the radius of a mathematical ellipse in general position. We need to recall two crucial facts about ellipses:

1. They have two *principal axes*, one the longest radius, one the shortest; these are at 90 degrees to each other, and are the ellipse's axes of symmetry.

2. In terms of the lengths d_1 and d_2 of the principal axes, the radius in any other direction is given by

$$d_\theta^2 = d_1^2 \cos^2\theta + d_2^2 \sin^2\theta,$$

where d_θ is the radius in the direction making an angle θ with the principal axis of length d_1. I use the letter d for the radii because they really stand for dilatations in the

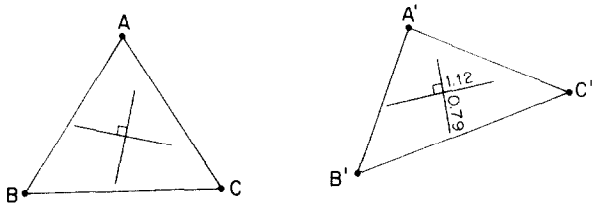

Fig. 9. The biorthogonal directions: axes of the ellipse from the previous figure, together with diameters of the circle transformed into those axes. One is along the direction of greatest rate of change of length; the other, along the direction of least rate.

transform of the triangles. One may restate properties 1 and 2 in terms more appropriate to our real interest, the geometry of transformation. Prefaced by "for homogeneous transformations of one triangle of landmarks into another," they become:

1′. There is a direction of greatest dilatation and a direction of least dilatation, and these are at 90 degrees both before and after the transformation.

2′. In terms of the principal dilatations, the rate of change of length in any direction is given by the formula at 2 above.

Since the circle of Fig. 8, *B* left is transformed into the ellipse of Fig. 8, *B* right, we need not draw many of the radii at all. Two will suffice—the principal axes, which correspond to principal dilatations, maximum and minimum. The orientation at which they lie upon the form is explicit in the drawing shown in Fig. 9.

What direction is this? Since we have no coordinate system available, we cannot describe it as "at 45 degrees to the horizontal" or even "at 45 degrees to edge *AB*," since that angle is not constant over the course of the change. Instead, we note that each arm of the cross is parallel to a line like *AG* (Fig. 6), connecting one of the vertices of the triangle to a point on the opposite edge. That point can be described by a fractional displacement from *B* toward *C*, a proportion which is the same in both triangles. By this device, we may position the crosses homologously upon the forms.

Recall from Fig. 7 that the directional dilatations we have computed apply at every point of the triangles. Any circle inside the abstraction which is the interior is taken into an ellipse exactly similar to that in Fig. 8. Then the particular circle we draw may as well be the largest, the *inscribed circle*, centered at the point equidistant from all three sides, the intersection of the triangle's angle bisectors. In the subsequent figures of this essay, the crosses of biorthogonal analyses are all centered and scaled in this manner to fit the triangles inside which they lie.

The principal axes and dilatations which correspond to the deformation of one arbitrary triangle into another may be computed by algebraically straightforward diagonalization of the affine derivative of the mapping, as explained in textbooks of tensor algebra. Alternatively, the axes may be explicitly constructed with ruler and protractor, and the dilatations directly measured as ratios of corresponding lengths, without any electronic aids. The seven-step construction is given in the Appendix to this article, along with a proof of its validity.

A note on the concept of "tensor"

The crosses displayed throughout this essay are pictures of *tensors*, coordinate-free representations of geometric change. A technical definition would be out of place here; the interested reader is referred to the gentle introduction in Lanczos'[7] course of lectures. In essence, a tensor is a geometric machine which takes a vector into another vector wholly without regard for coordinate systems. One may rotate or translate the coordinate system in which the vectors are measured; the output of a tensor machine will be transformed perfectly concordantly, translated or rotated right along with the observations. One will thereby arrive at the same ultimate quantifications (here, lengths and their ratios, the dilatations), however the cephalograms are laid down on the digitizer. Whatever the Cartesian coordinates by which the landmarks were archived, a tensor analysis, such as the biorthogonal method put forward here, will arrive at the same biometric conclusions.

III. INTERPRETATION OF CROSSES

The strength of biorthogonal analysis lies in its explicit display of crucial quantities inaccessible by conventional methods.

For instance, the analysis separates the observed change into one component for size change and a second for shape change. The product of the dilatations is the ratio by which the area of the triangle has increased; their ratio is a measure of the directionality of this size change, a measure the engineers call *anisotropy*. One may think of any distortion as the composition of two pure types: a pure size change, altering nothing but scale, of both principal dilatations $\sqrt{d_1 d_2}$; and a pure shape change, leaving area alone, of dilatation $\sqrt{d_1/d_2}$ along one arm and $\sqrt{d_2/d_1}$ along the other. This decomposition is sketched in Fig. 10.

An isotropic transformation, one which takes a triangle into a similar triangle, takes circles into circles. For these transformations, dilatations are equal in all directions, and the principal axes cannot be defined uniquely; any cross at 90 degrees will do (Fig. 11). As the transformation approaches isotropy, the orientation of the cross becomes more and more uncertain and

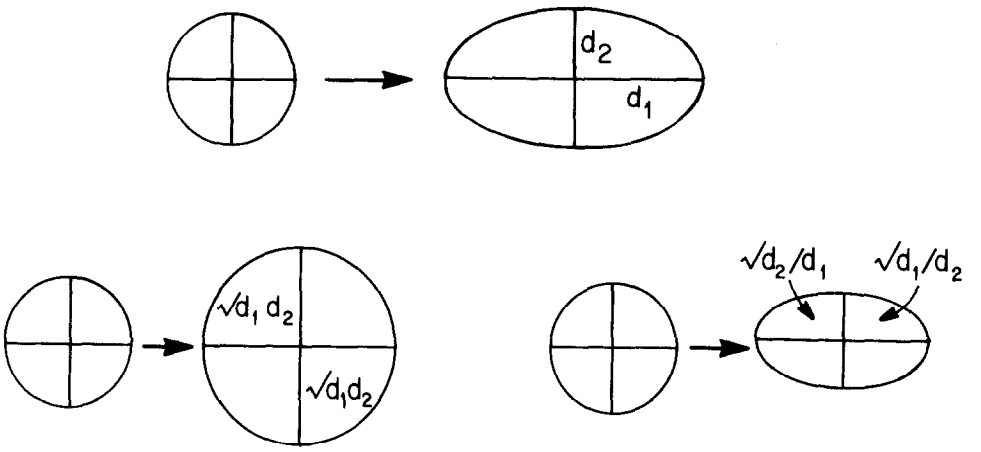

Fig. 10. The general transformation may be split into two components, a pure size change and a pure shape change.

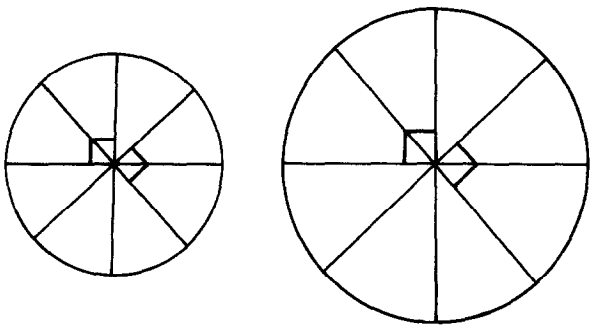

Fig. 11. The "principal axes" for an isotropic transformation are ambiguous.

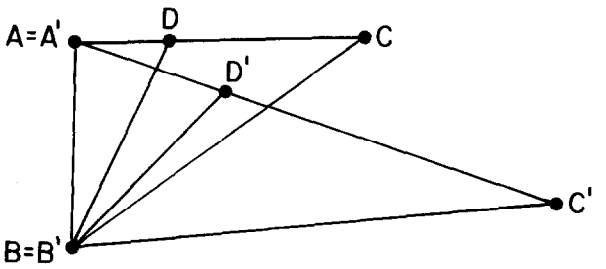

Fig. 13. A deformation leaving one side of a triangle unaltered in length usually involves a compression in some oblique direction. Although *AB* is fixed and *AC* and *BC* both grow greatly, length *B'D'* is shorter than its homologue *BD*.

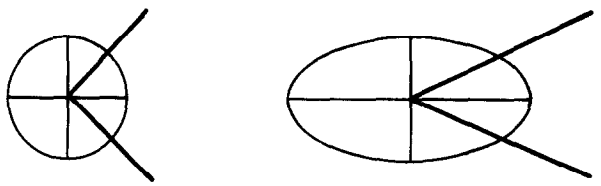

Fig. 12. Invariant proportions. The ratio of lengths placed symmetrically with respect to the biorthogonal axes is unaltered by the deformation.

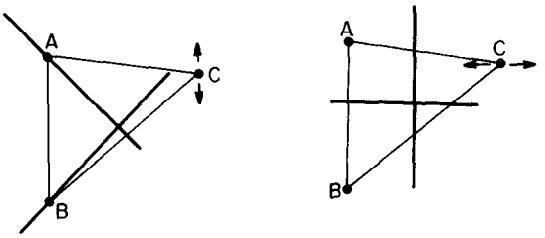

Fig. 14. Two special cases of biorthogonal analysis. **Left,** Apparent translation of *C* parallel to *AB* after scaling; axes at ±45 degrees to *AB*. **Right,** Apparent translation of *C* normal to *AB* after scaling; axes along *AB* and normal to it.

dependent upon measurement error. At the same time, since dilatations are virtually the same in all directions, it makes no difference where the cross is taken to lie. The cross bears only shape change information, and in the absence of shape change its orientation is not informative.

One arm of the cross is along the direction of largest dilatation, the other along the direction of smallest dilatation. These ratios are taken between images for distances along homologous segments. We can, instead, compute *proportions*, ratios computed within a single form. A change in proportion, as computed by taking ratios of homologously defined proportions, is equal to the quotient of the dilatations in the two directions which the proportion is comparing. Then, of all proportions within the triangle, that of distances along the major axis to distances along the minor axis increases fastest over the change, and its reciprocal increases most slowly (or decreases most quickly). Proportions

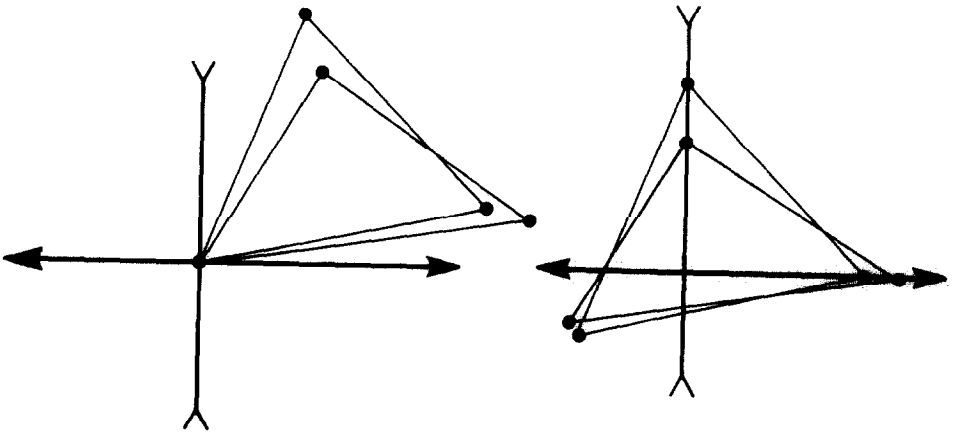

Fig. 15. Superpositions consistent with the biorthogonal directions for Fig. 7 to 9. Only the relative orientation of the images is determinate.

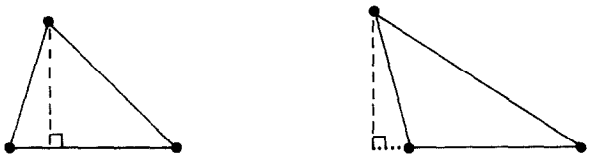

Fig. 16. Segments whose definition involves the construction of perpendiculars are not homologous; ratios of their lengths are not dilatations.

between pairs of directions placed symmetrically with respect to the prinicipal axes, as in Fig. 12, are invariant across the deformation.

The minimum dilatation cannot be greater than the dilatation observed for any edge of the triangle. If any edge is unaltered in length, there is likely to be a direction of compression oblique to it somewhere. In Fig. 13, one can be persuaded of this intuitively: the apparent "rotation" of edge AC about A should generate compression or extension toward or away from B. The precise principal direction takes into account the dilatation along AC in this connection. When, after registering on A and B, the apparent motion of point C is directly along AB (Fig. 14, left), then AB and its normal have the same unit dilatation, so that (in the limit of small changes) the principal axes are at 45 degrees between them. Only when C moves directly toward or away from the line AB are the principal axes of the deformation aligned with AB (Fig. 14, right).

When no side of the triangle is of fixed length, we can still scale the triangles with respect to each other, in any of three different ways, so as to make one edge appear to have dilatation 1. As the principal axes are not altered by any change of scale, the analysis of any observed deformation can be sketched as in Fig. 13 or its special cases. The "compression" is then relative to the correction of scale preceding the construction.

Biorthogonal analysis prescribes a mutual orientation for the two triangles: that for which the principal axes are aligned. We may draw this out, superposing at one of the vertices (Fig. 15, A) or at the internal intersection of two principal axes each running through one vertex (Fig. 15, B). In the rotation of homologous segments between the triangles we note the confusion sown for analysis by orienting on any single segment. This reorientation is not a "superposition rule," as registration is wholly arbitrary. As for segments (Fig. 4), any superposition at the correct orientation will correspond to a valid description of displacements out of some pair of algebraically homologous "centers" inside or outside the triangles. All such superpositions are misleading in their depiction of apparent motions of all the vertices, in which starting position is confounded with change.[6] (See the discussion of motion in connection with Figs. 19 through 21 below.) No superposition can be expected to be appropriate for more than three landmarks, one triangle, without explicit verification by means of the tensors.

The only right angle left at 90 degrees by a deformation is the angle between the principal directions. Other constructions involving right angles, such as the perpendicular projection of points to lines, are not homologous between triangles related by a deformation; one would not expect changes in related ratios to be explained in terms of the biorthogonal parameters. For instance, in Fig. 16 a projected distance reverses its directions, yielding a ratio of -1.0 between the forms, but the segments are not homologous, so the ratio is not a dilatation.

Even though constructions involving constant angles do not concur with the tensor analysis, we may infer changes in homologously measured angles. Angles with the axis of compression, or straddling it, as in Fig. 17, A, must open; those involving or straddling the

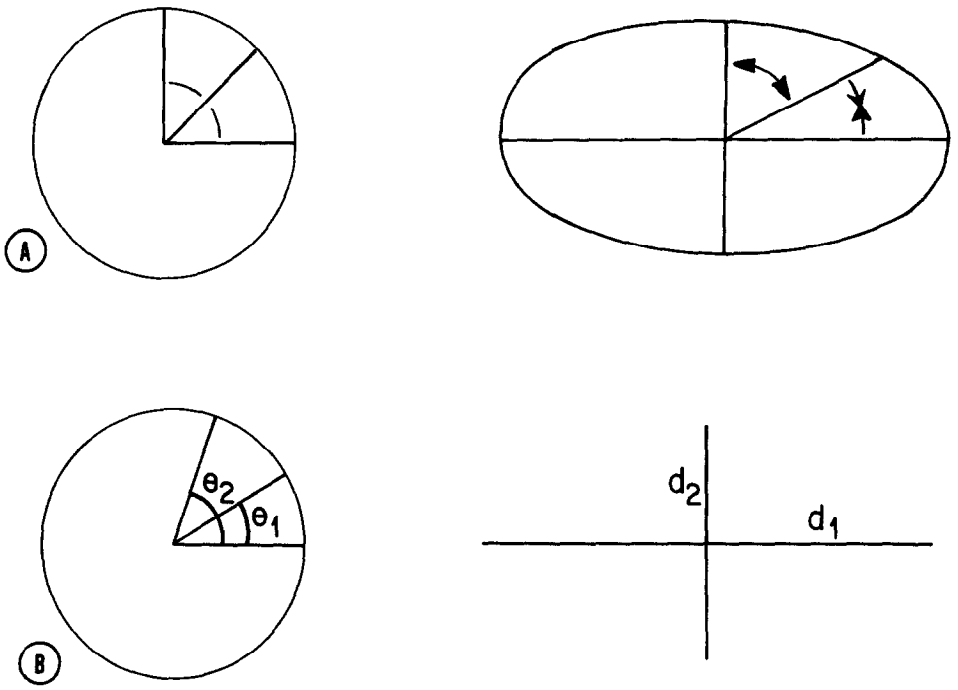

Fig. 17. The effect of deformation on measured angles is determined by the relation of the arms to the biorthogonal directions. **A,** Angles measured to the axis of relative compression open; those to the axis of relative extension close. **B,** Those angles are unchanged for which *tan* θ_1 *tan* $\theta_2 = d_2/d_1$.

axis of extension must shrink. Those which span both axes or neither will increase or decrease as the expanding or shrinking sector dominates. Analysis by way of the elementary trigonometric addition formulas, omitted here, indicates that those angles remain constant for which tan θ_1 tan $\theta_2 = d_2/d_1$ in Fig. 17, *B*. For small changes, where d_2/d_1 is very close to unity, these correspond to angles with $\theta_1 + \theta_2 = 90$ degrees—lines symmetrically placed about the bisectors of the principal axes. Conversely, where the arms of the principal cross make an angle of 45 degrees with the bisector of one of the triangle's angles, that angle will remain approximately constant over the shape change (Fig. 18).

The biorthogonal method thus directs our attention to two sorts of invariants among the landmarks themselves, without reference to fractions of displacement along the edges between. When a principal axis bisects a vertex angle, the ratio of the sides meeting there is invariant under the deformation; when a principal axis makes an angle of 45 degrees with that bisector, the angle measure at the vertex is (approximately) constant.

Although the description of change in terms of the motion of landmarks in a fixed coordinate system is not biometrically defensible (since superposition rules have neither biologic content nor empirical justification),[6] there is an alternative way for speaking of motion, founded in the biorthogonal analysis, which is sound. The principal axes through any vertex *C* of the triangle

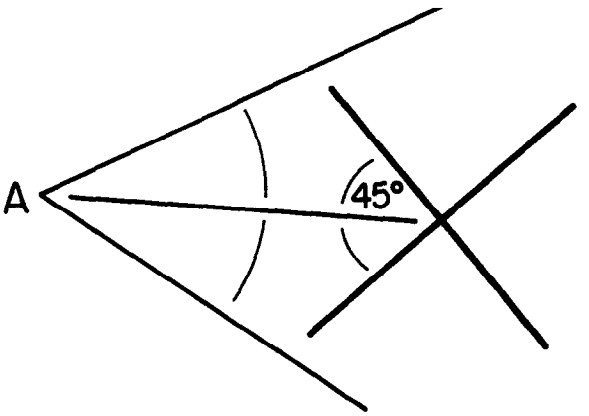

Fig. 18. If the biorthogonal axes lie as shown, then whatever the dilatations, as long as they are nearly equal, the angle at *A* will be very nearly constant.

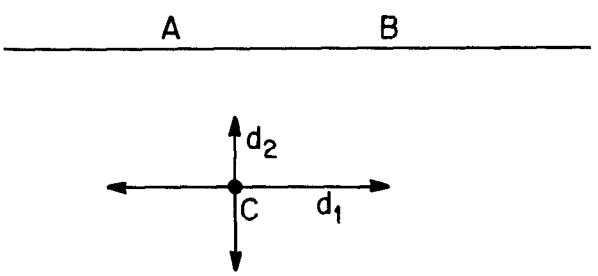

Fig. 19. "Motion" of a vertex with respect to the opposite edge. Case I. Axes aligned with that edge. The motion may be regarded as "toward" or "away from" the edge.

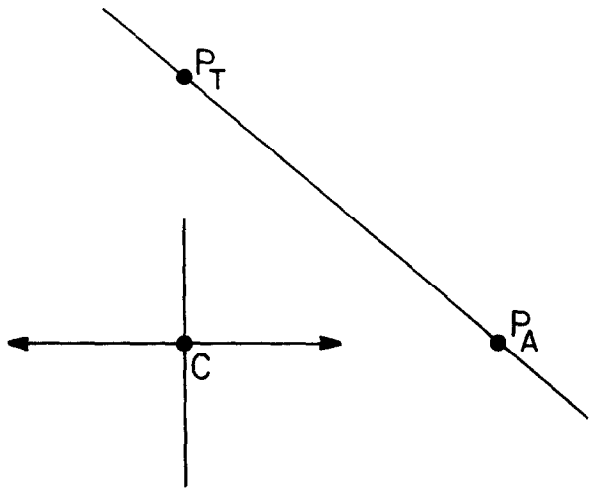

Fig. 20. Case II. Axes oblique to that edge. The motion may be regarded as toward one point P_T of the edge and away from another point P_A.

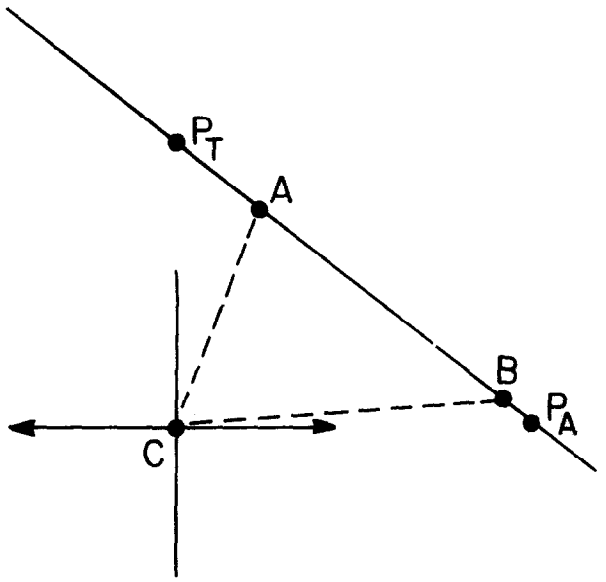

Fig. 21. Only when the other vertices *A* and *B* of the triangle lie inside the segment defined by the points P_T and P_A may we speak of vertex *C* as moving "forward" or "backward," away from *B* and toward *A* or vice versa.

ABC may be produced until they intersect the opposite side wherever they may, either between or outside the opposite vertices *A* and *B*. It may be that one of these intersections is "at infinity," if one principal axis is parallel to that opposite edge; then the other is perpendicular to that edge, as in Fig. 19, so that point *C* is growing "straight toward" or "straight away from" edge *AB*. Otherwise (Fig. 20), point *C* is "moving toward" one point P_T on this edge and "moving away from" another point P_A. This description has explicitly

Fig. 22. Unsuitable triangles with one side or one altitude too short. In the presence of small errors of landmark location, the computed principal axes will tend to lie along these directions.

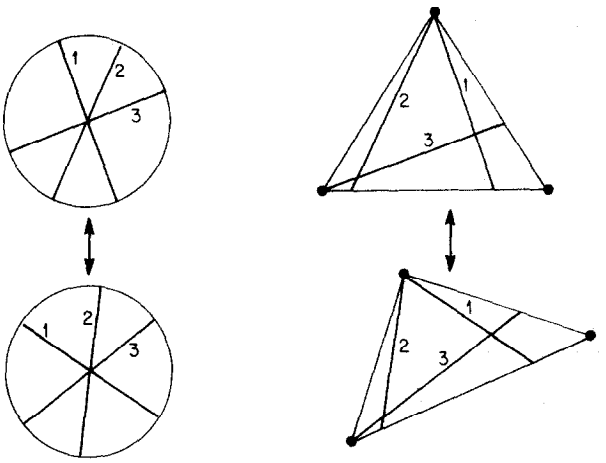

Fig. 23. The homology function by which we coordinate transformations of different triangles is one version of the homology between segments before and after deformation of a single triangle. "Direction" is specified by fraction in which a segment through a vertex divides the opposite edge internally. Note the irregularity of the correspondence of directions *1*, *2*, and *3* considered as a function of angle.

taken into account dilatations along the edge *AB*, correcting the major fallacy of the vector displacement methods. Only if the intersections with principal axes through *C* both fall outside the opposite edge, as in Fig. 21, is the rate of dilatation from *C* steadily increasing or steadily decreasing in passing from *A* to *B*. Only in this case can one speak of *C* as moving away from *B and* toward *A*, or vice versa. For instance, we learn from Fig. 15 (compare with Fig. 21) that in Fig. 9 point *B* has moved away from *C* and toward *A*. But in any set of three vertices at two times, one is moving toward a point between the other two, and one away; neither of these two may be described as moving "forward" or "backward" with respect to the opposite edge in this way.

(Triangles of one angle nearly 0 or nearly 180 degrees are unsuited to this form of analysis. For these triangles, the range of absolute lengths among homologously definable segments is too great; either one side or one altitude, Fig. 22, is very short relative to the general scale of the figure. Small errors of either homology or digitization will disproportionately affect

dilatations along these smaller segments, so that one of the principal axes will tend to lie along the short direction. There is no real harm done in excluding these triangles from analysis, as their area is very small.)

The appropriate polarity for description of shape change is not horizontal/vertical (the language of coordinates) but, rather, stretch/shrink, the language of tensors. The former approach, which demands the unnatural imposition of a coordinate system common to two forms, leads directly to the confusion of superpositions upon a coordinate frame (a two-point registration-orientation) which is itself dilating. The relation of point to line, if changing, is expressed not by the vector of displacement but by the tensor of deformation—two rates of change in two orthogonal directions. That one of the landmarks may be osteologically fixed (for instance, sella) or incapable of any action at all (such as a metallic implant) is of no immediate relevance for morphometrics. Only after a description is made consistent, unambiguous, and geometrically meaningful is it appropriate to inquire of the organism how it brought about the change now clearly observed.

The description of shape change and the description of shape are conceptually quite independent. Shape is a matter of the archive—not measured "shape variables" but positions of landmarks with respect to each other or to axes. Shape change is very different. It is a tensor expressing directionality of dilatation; its descriptor, the biorthogonal cross, resembles not at all a simple contrast of coordinates or interlandmark distances taken from archives of forms separately. However, from its empirical form we may deduce optimal measures of contrast or invariance to make most effective use of the raw information stored in those archives.

IV. AVERAGING

A crucial element of any cephalometric system is its mode of summary over cases. As expounded so far, the biorthogonal method examines the deformation of one particular triangle into another. We must extend the analysis to populations of shape changes.

One can imagine several ways in which variation might be introduced into the simple descriptive scheme of the single cross. In the basic diagram (Fig. 9) we might vary the starting positions of the landmarks with respect to each other, or we might vary their orientation with respect to the grid; we might vary the dilatations of the grid by random adjustments of the ratios; we might randomly displace the landmarks after deformation; or we might vary the transformation spatially, using different dilatations and orientation at each point, so that lines straight in one form are homologous to curves in the other. This last possibility corresponds to the method of biorthogonal grids, which I have presented in some detail elsewhere for the study of particular histories case by case.[4, 5] The other alternatives all correspond to particular sorts of averaging, particular presumptions of "error variance." In this article I suggest a new method that is a great deal simpler than any heretofore have been.

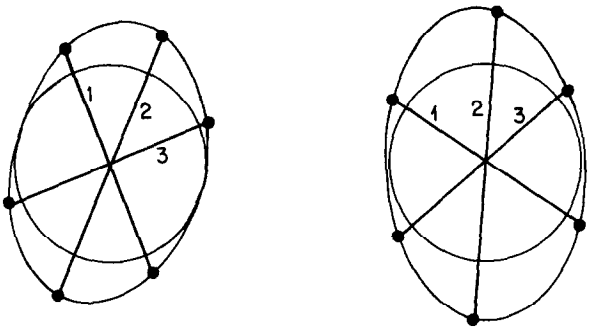

Fig. 24. Correspondence function for dilatations from two transformations. The ellipses are assumed to depict the strains relating the triangles of Fig. 23 to two others, not shown.

The same linear correspondence (Fig. 8, *A*) that permits us to note homologies of segments in pairs of forms allows us as well to note homologies of dilatation in pairs of changes. We may *define* homology of direction in different forms, whether or not related by growth, by equality of the fractions in which segments through a vertex divide the edges opposite (Fig. 23). This is not an even correspondence with respect to angles at the center of the ellipse; it requires the triangles for its computation. Two strain ellipses representing dilatations for two shape changes are two functions of direction on a circle. We can set their arguments into correspondence in terms of this convenient vertex-based homology between the segments they represent (Fig. 24).

Proceeding in this manner, we may accumulate many of these ellipses, all labeled homologously, corresponding to many observed deformations between pairs of triangles. Now, finally, we have the stuff of classic statistics: a "measurement vector" in the usual insubstantial "measurement space." We can average the dilatations of each homologous family to arrive at an average rate of change of length in that direction; we can report, too, the variance of the sample of dilatations around this average, direction by direction. To the extent that the strain ellipses being averaged are consonant, the mean dilatations will fairly well describe another ellipse, the "average" strain (Fig. 25), which will have a unique direction of maximum dilatation and a unique direction of minimum dilatation at roughly 90 degrees to each other. In every case the "directions"

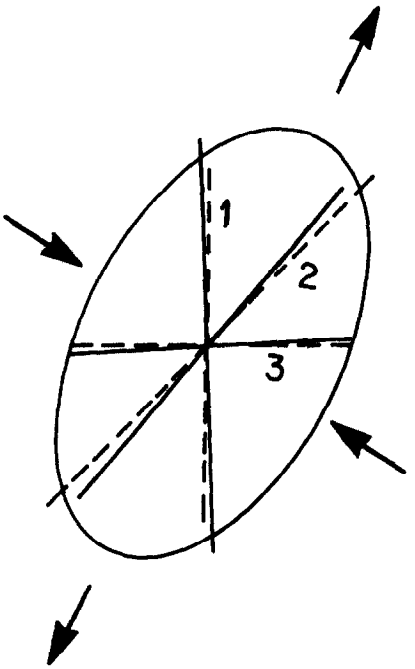

Fig. 25 The strain that is the average of the two shown in Fig. 24, and its principal directions. They will tend to lie between the principal directions of the component strains. Dashed and solid lines should lie exactly atop each other, but have been rotated slightly for clarity.

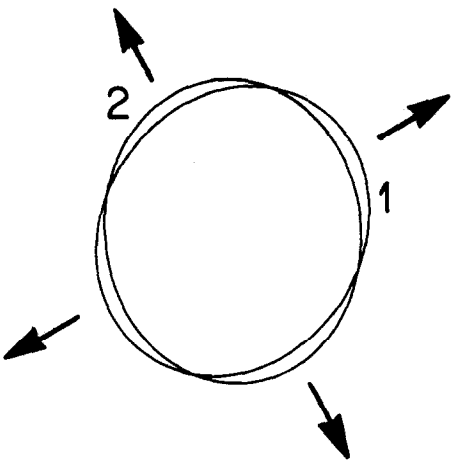

Fig. 26 The relative strain for a pair such as that in Fig. 24, representing quotients of corresponding dilatations, and its principal directions.

are specified by the fractions in which segments through a vertex divide the edge opposite (Fig. 23).

Likewise, from two ellipses of dilatations, we may compute the ratio *between* them, direction by direction. The resulting pattern of ratios will approximate to the radii of yet another ellipse, in particular manifesting a

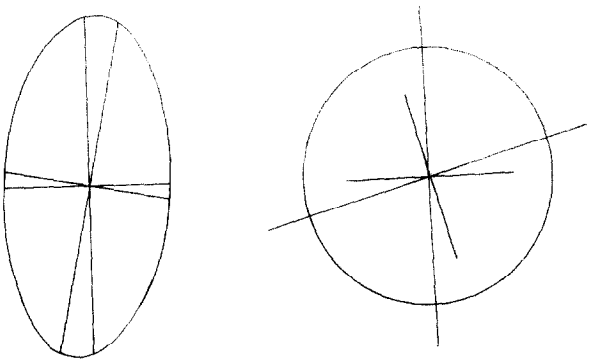

Fig. 27. The amount of individual anisotropy preserved in the mean tensor varies inversely with the scatter of principal directions.

direction of greatest ratio and a direction of least ratio at approximately 90 degrees once again, as illustrated in Fig. 26. These directions represent extremes of relative mean dilatation, the excess (or deficit) of growth in the one group relative to the other. We will use this formalism to speak of treatment effects upon "normal" growth in Section V.

In this manner, we characterize both mean shape changes and mean difference in shape change using the same biorthogonal formalism by which we parameterized the individual shape changes themselves.

In the computation of mean tensors there emerges an interesting ancillary statistic. Recall that for each shape change there is a measure of anisotropy, the comparison of the greater principal dilatation with the lesser. If all the crosses for all the shape changes of a population are aligned in the same direction, the maximum dilatation in mean would be the mean of the separate maxima, and likewise the minima. The anisotropy of the mean change would then be just the mean of the anisotropies of the separate shape changes being averaged. It cannot be larger than that, but it can be smaller. If the directions of extreme dilatation for the individual deformations wander from an accurate mutual alignment, then the average will mix dilatations along extremal directions of certain shape changes with middling dilatations of others (Fig. 27), whereupon the observed maximum and minimum mean dilatations would be attenuated toward the mean from the scores had the individual shape changes been aligned. The ratio of anisotropy in mean to mean anisotropy is a useful statistic, a sort of fraction of variance explained by shape change. Should it be high, the shape component of the mean transformation is a good representation of the individual shape components contributing to it, both in anisotropy (maximum change in proportions)

and in direction. Where the ratio is low, then even though individual shape changes may be highly directional, their principal axes wander so that at best only the isotropic component, direction-free size increase, is of any consistency. Such a degradation of geometric information may be due to heterogeneity of the population, intrinsic variability of the growth process, or use of nonhomologous "landmarks."

A note on computation: It would be possible to compute the maxima and minima of these mean dilatations by exact algebraic manipulations, iterative and slow. It is easier to approximate them via a sample of the dilatations for sixty distinct classes of homologous orientations. The computer program used in the examples of this article divides each side of each triangle into even twentieths and connects each division to the opposite vertex. Along each of these sixty paths a dilatation is computed, for each shape change of a population, as the express quotient of homologous lengths. From the averages of homologous dilatations, as from the ratios of those averages, the maximum and minimum are selected directly. The accuracy with which these empirical extremes lie at 90 degrees in the figures is limited by the discreteness of orientations from which this procedure selects and by deviations from ellipticity in averages from heterogeneous populations of shape change.

The analysis proposed here for a single pair of triangles is fully equivalent to the simplest case of the *finite-element* description, a formalism familiar in other branches of biomechanics and central to the computation of my extended biorthogonal grids. However, the finite-element literature seems nowhere to have considered the problem of averaging over whole populations changing their shapes. The expert may straightforwardly generate alternative procedures—for instance, averaging shapes rather than shape changes, or mapping all deformations upon a "standard." In such approaches the computed mean, although arbitrary in certain crucial particulars, will be an exactly linear map itself with principal strains at exactly 90 degrees. As I was unable to extend this use of proper tensors to the description of comparisons between groups, I chose not to emphasize the finite-element formalism in the presentation here.

V. ORTHODONTIC TREATMENT EFFECTS ON CRANIOFACIAL GROWTH

Over a decade of innovation, Dr. Sheldon Baumrind and several colleagues[1–3] have created a discipline that might be called "cephalogrammetry," the study and optimization of precision in cephalometric data collection. They have shown us how to screen effectively for random errors in locations of landmarks; they demonstrate, for change scores, the elimination of nonhomology (the main source of systematic error) by using each tracing as a superimposable verification of the others; and they show how landmarks have individual statistical quirks which can be used to advantage in operational definitions and in analysis.

A major effort of Baumrind's group has been the collection and exhaustive preparation of a canonical data base embodying the best-known procedures for all of these concerns. The data base is designed in the form of a quasi-experiment to assay effects of Class II treatment, with a control group and several populations subjected to various therapeutic tactics. Assignment of treatments could not, of course, be randomized. Rather, Baumrind sought out clinicians, regarded by their colleagues as experts, who favored one style of Class II therapy; he then extracted random samples of case histories from their records. As it happens, at the outset of treatment the groups are not meaningfully different from each other or from a control group, drawn from other sources, of untreated cases of the Class II form.

For this study I use three of the six groups reported in Baumrind's most recent analysis: control, cervical, and intraoral. (See Baumrind et al.[3] for the operational definition of the treatment groupings.) Each case of control is represented in the data by a pair of films taken at an interval averaging 24 months.

Baumrind's research group has grappled with the stubborn problem of comparing changes of different duration. For the reanalysis here, I copy without comment the technique they adopted. We annualize all observed changes by computing increment per year or percent increment per year. For this reason, we exclude cases with relatively very long or very short elapsed time between films (in this data set, fewer than 12 months or more than 42 months).

Dr. Baumrind kindly made available to me Cartesian coordinate pairs, film by film, of the seven landmarks on which his most recent publications are based: nasion, sella, condylion, gonion, menton, pogonion, and anterior nasal spine. I shall abbreviate them here by their initials, N, S, C, G, M, P, and A. For the seven landmarks we can construct thirty-five triangles, each of which manifests a mean shape change for each of the three groups.

Consider a typical triangle formed from these landmarks, the triangle S-P-A. It represents no particular hypothesis, as its vertices lie on three different bones. The graphic output of a biorthogonal analysis of

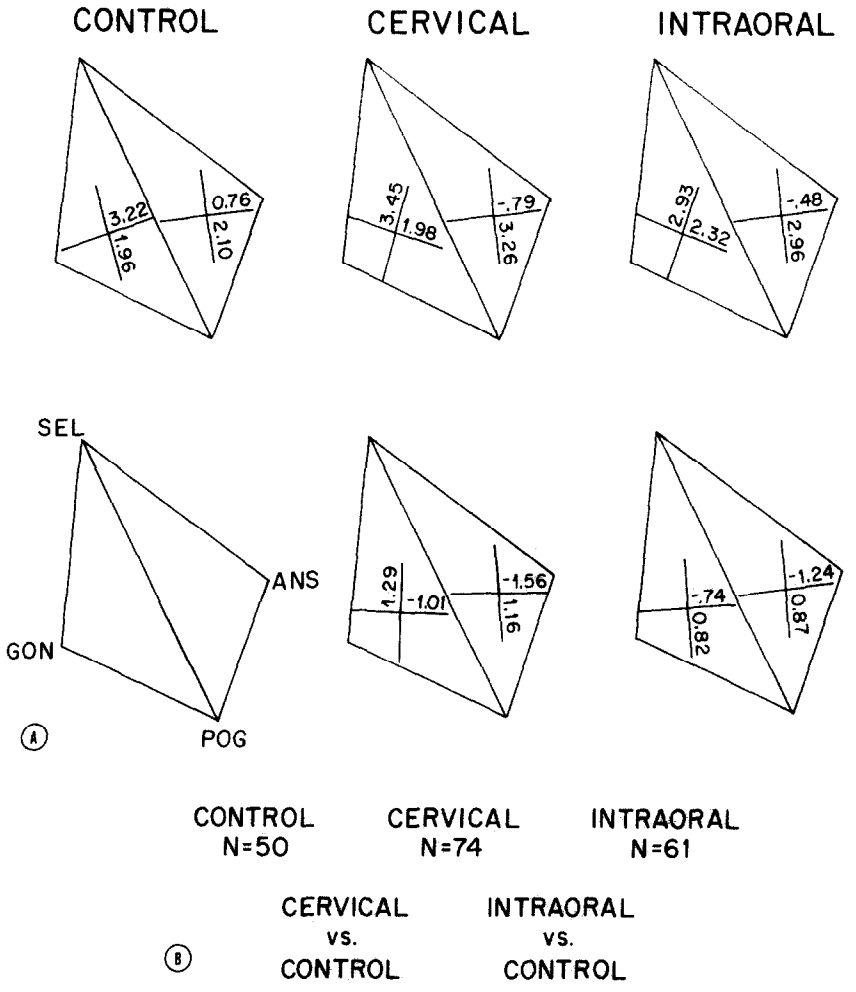

Fig. 28. A, Typical graphic output of a biorthogonal analysis; principal directions and dilatations of group means and of comparisons among group means for multiple triangles. The particular shape drawn is the control group "pretreatment" mean, coordinate by coordinate, according to a sella-nasion registration. **B,** Legend for the five frames of panel **(A)** and subsequent figures.

this or another single triangle over the groups may be conveniently arranged into a little matrix of two rows and three columns (Fig. 28, *A*), the cells of the matrix corresponding to means and comparisons of means as identified in Fig. 28, *B*. For reasons which will become clear shortly, this triangle is displayed together with another, S-P-G, in a sort of mosaic: two triangles with one shared edge.

The actual form drawn (the abstraction upon which the crosses are laid down) is the triangle of centroids of the original coordinate locations, landmark by landmark, for the "pretreatment" films of the control group. For this construction to be legible, films must have been digitized in a consistent orientation (here, sella-nasion). Such assignment of a coordinate system, necessary to realize the diagrams, does not affect the biorthogonal computation in any way.

By way of examining the parameters shown in Fig. 28, *A*, let us consider first the panel at upper left, the control history. This is the depiction of the average distortion among the "cases" of this group in terms of the maximum and minimum of mean dilatation over sixty classes of homologous segments. The observed maximum is 2.10, representing an increase of 2.10 percent per year in the direction from pogonion to a point 0.55 of the way from sella to ANS; the observed minimum represents an increase of only 0.76 percent per year in the direction from ANS to a point 0.45 of the way from pogonion to sella. (For the computation of those fractions 0.55 and 0.45, see Fig. 29). These directions ought to be approximately orthogonal in most of the sample triangles. The dilatations are given in printed form in Fig. 30, in the entry for triangle 3. The table reports standard errors for each of these means;

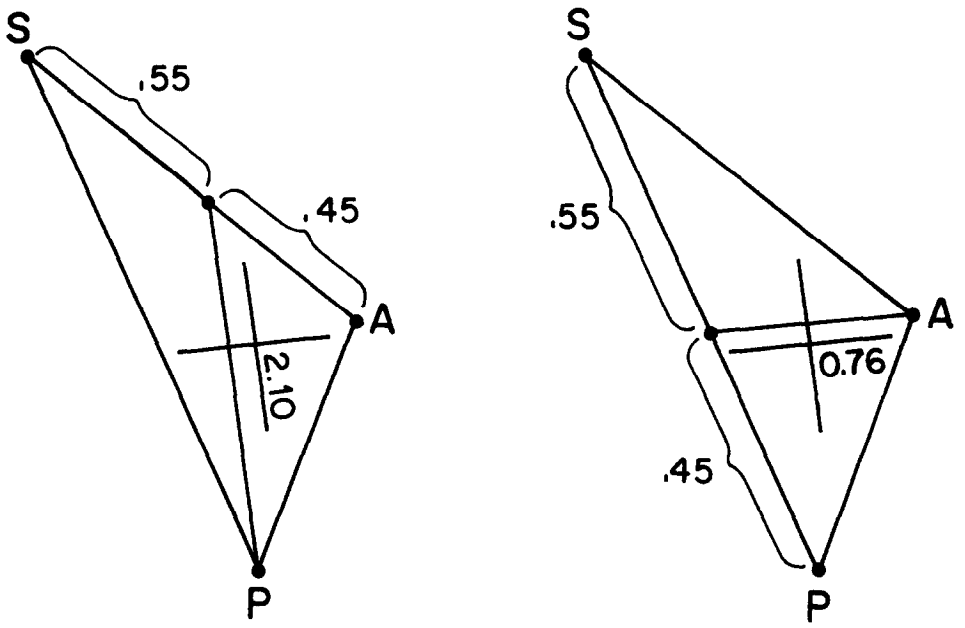

Fig. 29. Determining the descriptions of the grid directions as drawn.

for instance, the standard error of the figure 2.10 percent per year is 0.12 percent per year. The difference between 2.10 percent and 0.76 percent is an anisotropy in mean of 1.34 percent per year greater growth in one direction than in the other. For the individual triangles whose analysis was pooled here, the mean of the corresponding *individual* anisotropies was 2.54 percent per year. Then for S-P-A the mean shape change explains 1.34/2.54 = 53 percent of the net individual shape change, independent of size change. This corresponds to a distribution of directions midway between the extreme cases of Fig. 27.

Passing to the right along the top row, we discover principal axes for the treatment groups which are perfectly aligned (to the 0.05 fractional spacing this computation relies on) with those we just noted for the controls. The dilatations in these directions, however, are altered. Each treatment group shows additional annualized *extension* along the line of greatest extension for the controls (3.26 percent or 2.96 percent versus 2.10 percent) and *reduction* along the line of least extension for the controls (−0.79 percent or −0.48 percent versus +0.76 percent). For the cervical group, this triples the mean directionality of growth, from 1.34 percent to 4.05 percent. In this group the triangle S-P-A grows, on average, 4 percent per year faster vertically than horizontally, the greatest such contrast to be found anywhere in the data set.

Because growth under treatment is aligned in the same directions as control growth for this triangle, the treatment effects are aligned in the same directions. Their "relative dilatations," the algebraic differences of treatment and control dilatations, are presented in the bottom row of the figure, where each tensor contrast with control growth is drawn under the treatment group mean. For instance, the relation of cervical growth to control growth is shown in the middle of the bottom row. It consists of distortion by an additional 1.16 percent per year of vertical extension and a shortfall of 1.56 percent per year horizontally. ("Vertical" and "horizontal" are defined here with respect to the coordinate system of the diagram, oriented on sella-nasion). Under the heading "principal relative dilatations" the tabulation in Fig. 30 repeats these two quantities and indicates their approximate standard errors. The horizontal effect, −1.56 percent, is −4.5 times its standard error of 0.34; the vertical effect, 1.16 percent, is five times its standard error of 0.23 percent. Some sort of significance test is appropriate here, perhaps a *t*-ratio corrected for our having selected the extremes of observed contrasts.

The effect of the intraoral treatment is the same as that for the cervical treatment except in magnitude: 1.24 percent per year horizontal shortfall versus 1.56 percent, 0.87 percent per year vertical extension versus 1.16 percent.

Let us turn now to S-P-G, the other triangle depicted in Fig. 28, *A*. For the controls (upper left panel), the principal directions of mean shape change are roughly parallel to those for S-P-A, but their polarity is

Control N = 50	*Cervical* N = 74	*Intraoral* N = 61

Triangle 1, SEL-ANS-MEN

Anisotropies

1.370< 2.386> 3.891< 4.486> 3.192< 3.516>

Principal dilatations

2.075(0.109)	3.234(0.177)	2.866(0.121)
0.706(0.199)	−0.657(0.250)	−0.326(0.188)

Principal relative dilatations

1.181(0.22)	0.806(0.17)
−1.388(0.32)	−1.057(0.27)

Triangle 2, SEL-GON-MEN

Anisotropies

1.750< 2.350> 1.239< 2.178> 0.511< 2.240>

Principal dilatations

3.735(0.188)	3.486(0.197)	3.004(0.164)
1.986(0.112)	2.246(0.192)	2.493(0.157)

Principal relative dilatations

1.294(0.21)	0.811(0.17)
−1.231(0.28)	−0.982(0.30)

Triangle 3, SEL-ANS-POG

Anisotropies

1.339< 2.539> 4.045< 4.742> 3.442< 3.928>

Principal dilatations

2.100(0.117)	3.255(0.188)	2.964(0.160)
0.762(0.220)	−0.790(0.285)	−0.478(0.206)

Principal relative dilatations

1.165(0.23)	0.866(0.21)
−1.557(0.34)	−1.240(0.30)

Triangle 4, SEL-GON-POG

Anisotropies

1.263< 2.056> 1.473< 2.289> 0.617< 2.124>

Principal dilatations

3.223(0.153)	3.453(0.189)	2.933(0.142)
1.959(0.103)	1.980(0.166)	2.316(0.156)

Principal relative dilatations

1.295(0.22)	0.825(0.17)
−1.006(0.24)	−0.737(0.25)

Triangle 5, CON-ANS-MEN

Anisotropies

0.854< 2.047> 3.349< 4.079> 2.561< 3.192>

Principal dilatations

2.044(0.132)	3.303(0.197)	2.900(0.154)
1.190(0.195)	−0.047(0.213)	0.339(0.167)

Principal relative dilatations

1.316(0.24)	0.894(0.20)
−1.293(0.29)	−0.889(0.26)

Triangle 6, CON-GON-MEN

Anisotropies

2.094< 3.445> 1.505< 3.556> 0.324< 3.547>

Principal dilatations

3.785(0.259)	3.746(0.295)	2.815(0.309)
1.691(0.217)	2.241(0.207)	2.492(0.194)

Principal relative dilatations

1.809(0.37)	1.072(0.35)
−1.244(0.34)	−1.164(0.41)

Triangle 7, CON-ANS-POG

Anisotropies

0.783< 2.187> 3.434< 4.231> 2.740< 3.521>

Principal dilatations

2.063(0.131)	3.326(0.201)	3.013(0.197)
1.280(0.219)	−0.108(0.237)	0.274(0.169)

Principal relative dilatations

1.286(0.25)	0.962(0.24)
−1.404(0.31)	−1.021(0.28)

Triangle 8, CON-GON-POG

Anisotropies

1.472< 2.877> 1.657< 3.414> 0.499< 3.138>

Principal dilatations

3.159(0.209)	3.628(0.286)	2.776(0.273)
1.687(0.217)	1.970(0.186)	2.277(0.210)

Principal relative dilatations

1.794(0.36)	1.068(0.34)
−0.996(0.29)	−0.850(0.31)

Triangle 9, SEL-ANS-GON

Anisotropies

0.876< 1.844> 3.056< 3.358> 2.241< 2.576>

Principal dilatations

2.326(0.104)	3.417(0.180)	2.906(0.128)
1.450(0.104)	0.361(0.177)	0.665(0.126)

Principal relative dilatations

1.321(0.22)	0.817(0.19)
−1.310(0.23)	−1.023(0.19)

Triangle 10, CON-ANS-GON

Anisotropies

0.576< 2.212> 2.950< 3.768> 1.887< 2.955>

Principal dilatations

2.075(0.131)	3.488(0.252)	2.783(0.249)
1.498(0.212)	0.538(0.165)	0.895(0.112)

Principal relative dilatations

1.731(0.33)	1.068(0.34)
−1.280(0.23)	−0.965(0.19)

Triangle 11, MEN-ANS-GON

Anisotropies

1.315< 2.180> 2.369< 3.090> 2.050< 2.834>

Principal dilatations

2.851(0.143)	3.319(0.219)	3.115(0.173)
1.536(0.145)	0.950(0.177)	1.066(0.132)

Principal relative dilatations

1.128(0.28)	0.815(0.23)
−1.273(0.21)	−1.010(0.19)

Triangle 12, POG-ANS-GON

Anisotropies

1.031< 2.069> 2.409< 3.152> 2.204< 3.114>

Principal dilatations

2.686(0.134)	3.359(0.237)	3.270(0.228)
1.655(0.161)	0.949(0.176)	1.066(0.133)

Principal relative dilatations

1.115(0.32)	0.913(0.29)
−1.185(0.20)	−0.944(0.19)

Triangle 13, NAS-SEL-ANS

Anisotropies

1.326< 1.849> 2.594< 3.128> 1.529< 2.266>

Principal dilatations

2.448(0.140)	3.457(0.253)	2.375(0.169)
1.122(0.080)	0.863(0.119)	0.846(0.057)

Principal relative dilatations

1.119(0.30)	−0.063(0.25)
−0.347(0.17)	−0.294(0.12)

Triangle 14, NAS-SEL-MEN

Anisotropies

0.999< 1.636> 2.037< 2.474> 1.880< 2.252>

Principal dilatations

2.142(0.098)	3.182(0.160)	2.738(0.104)
1.142(0.074)	1.145(0.121)	0.857(0.072)

Principal relative dilatations

1.041(0.19)	0.640(0.14)
0.003(0.14)	−0.313(0.12)

Fig. 30. (For legend, see opposite page.)

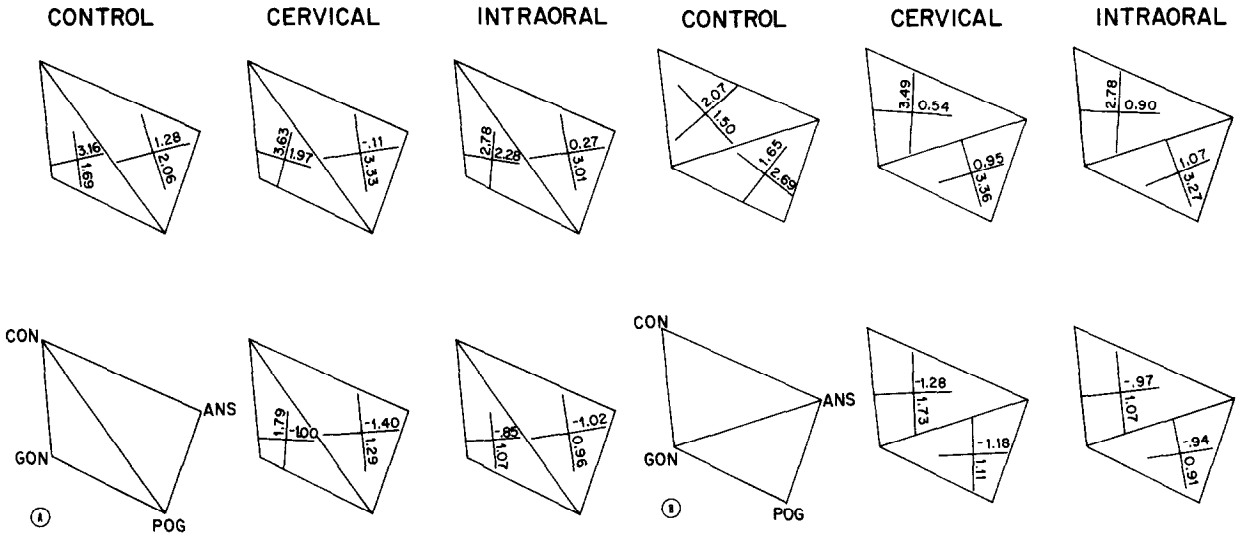

Fig. 31. Five other mosaics drawn from the polygon sella-ANS-pogonion-menton-gonion-condylion. The tensors of the lower row—biorthogonal analyses of the treatment effects—are oriented uniformly vertical and horizontal in all these triangles. At the upper right of frame *C* note the isotropy of changes in the triangle Con-Gon-Men under intraoral treatment. The range between maximum and minimum mean dilatations is only 0.32 percent per year. Even though the average mandible in this group is altered by some 3.5 percent per year more in one direction than in another (Fig. 30, triangle 6), these directions are not stable enough in the group of cases collected here to be of any use in treatment planning.

reversed; the direction of greatest extension in S-P-G (3.22 percent per year) is aligned with that of least extension in S-P-A (0.76 percent per year). In the treatment groups, by contrast, the polarities are in accord, but the directions of maximum or minimum dilatation under treatment are rotated by some 25 degrees from those for the controls.

Nevertheless, we may still invoke the procedure of Fig. 26 to compute descriptions of the treatment changes relative to the control changes. The resulting quotient is aligned with neither of the two mean changes but is, instead, most gratifyingly aligned with the relative axes for S-P-A, the other triangle we first examined. The treatment effects are geometrically parallel, even though the composites of treatments by normal growth are skew. For this second triangle, S-P-G, the principal decrease in expected change in length owing to either treatment is horizontal, about 1 percent per year, and the principal increase is vertical, about 1 percent per year. The effect of intraoral treatment is again roughly proportional to the effect of cervical treatment, with coefficients one-fifth to one-third smaller. The differences between corresponding relative dilatations for the two triangles are insignificant in the vertical direction and possibly significant (but probably not interpretable) in the horizontal direction. Clearly, the treatments have more in common than they have in contrast.

Note that none of the finite vectors between landmarks of the mosaic run either vertically or horizontally. The optimal contrasts (effects) that we are measuring lie in directions that are inaccessible to the conventional analyses based on these same data.

For the polygon S-C-G-P-M-A, excluding nasion,

Fig. 30. Statistics for the analysis of fourteen triangles from Baumrind's data base. For each triangle, under "anisotropies" are the differences between maximum and minimum mean dilatations for each group and, in brackets, the corresponding mean difference of the individual maximum and minimum dilatations. The ratio of these is "variation explained by shape change." Under "principal dilatations" are the numbers written upon the crosses of the upper row of triangles—extrema of mean dilatation over sixty directions—and, in parentheses, their standard errors. Under "principal relative dilatations" are the extrema of quotients of mean dilatation over the sixty directions for the comparison of each succeeding column with the first and, in parentheses, the approximate standard errors imputed to those differences by sample variation alone.

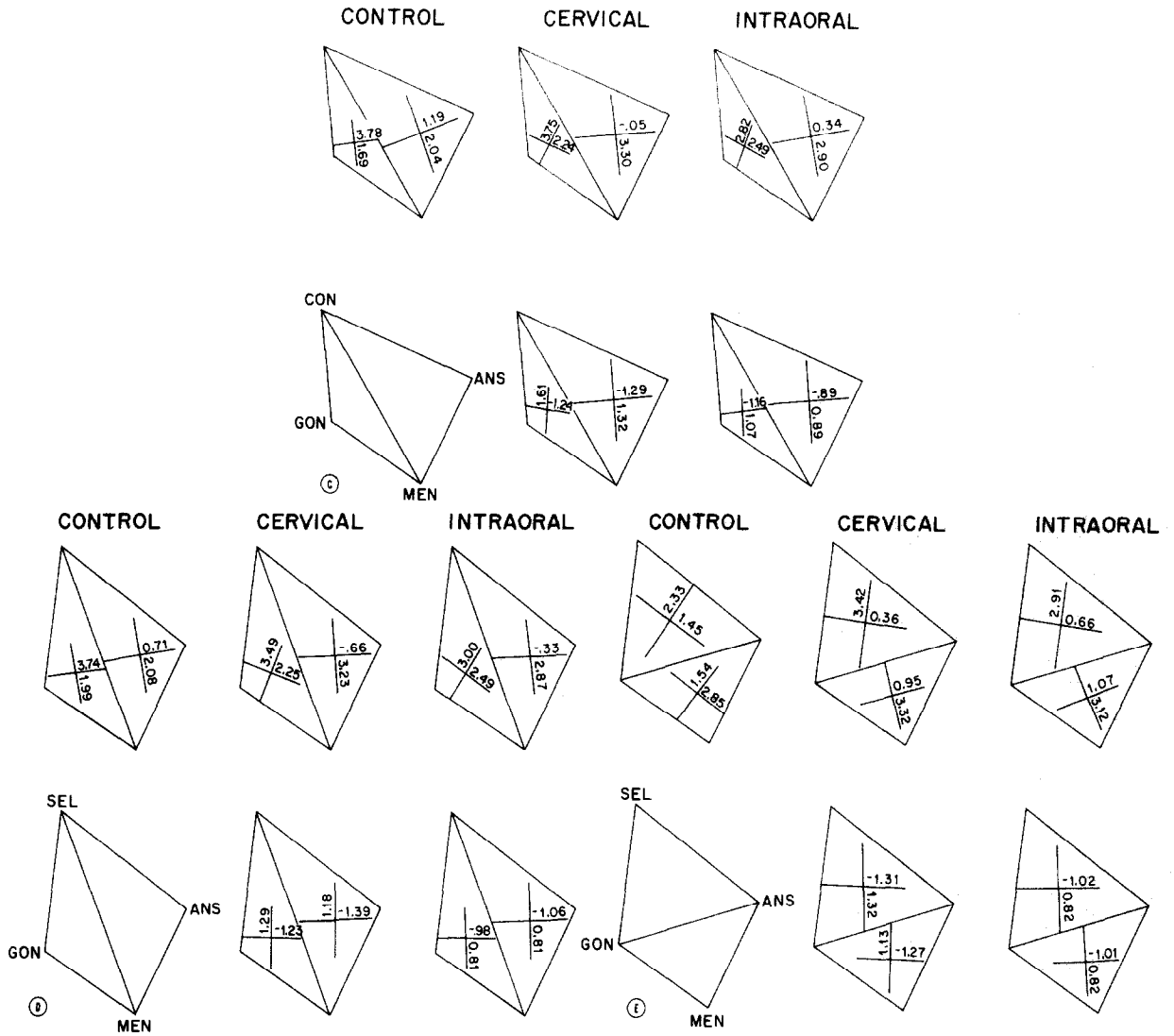

Fig. 31 Cont'd. (For legend, see page 193.)

there are ten other triangles, five other mosaics, which do not involve unsuitable triangles on edges S-C or M-P. The biorthogonal summaries for all ten, displayed in Fig. 31, are consistent with the same description of the treatment effects extracted from Fig. 28. Beyond the changes attributable to control growth, there is extension vertically at the rate of some 1.0 to 1.5 percent per year for cervicals, somewhat less for intraorals, and relative reduction horizontally at the same rates. Small local deviations (for instance, the dilatation along C-G, which is about 1.8 percent per year in the cervicals, versus only 1.3 percent along S-G) do not distort the underlying pattern. For these three groups of Baumrind's, the biorthogonal analysis of the six-point polygon is simple, consistent, and clear.

Data for the seventh of Baumrind's landmarks, nasion, suggest a different scheme of directional dilatations. The most convenient triangle for examining them is S-N-A, the smallest triangle involving nasion. In Fig. 32, *A* we see that for controls the deformation of this triangle due to growth is approximately along vertical and horizontal principal axes, with 1.3 percent per year more dilatation vertically than horizontally. For the intraorals, the change in this triangle is almost the same. But for cervicals, the anisotropy is doubled, from 1.33 percent per year to 2.60 percent, and the principal directions have altered. In the bottom center panel we note the additional expansion of the distance of nasion from the sella-ANS line by 1 percent per year, a relative dilatation which is just about zero in the

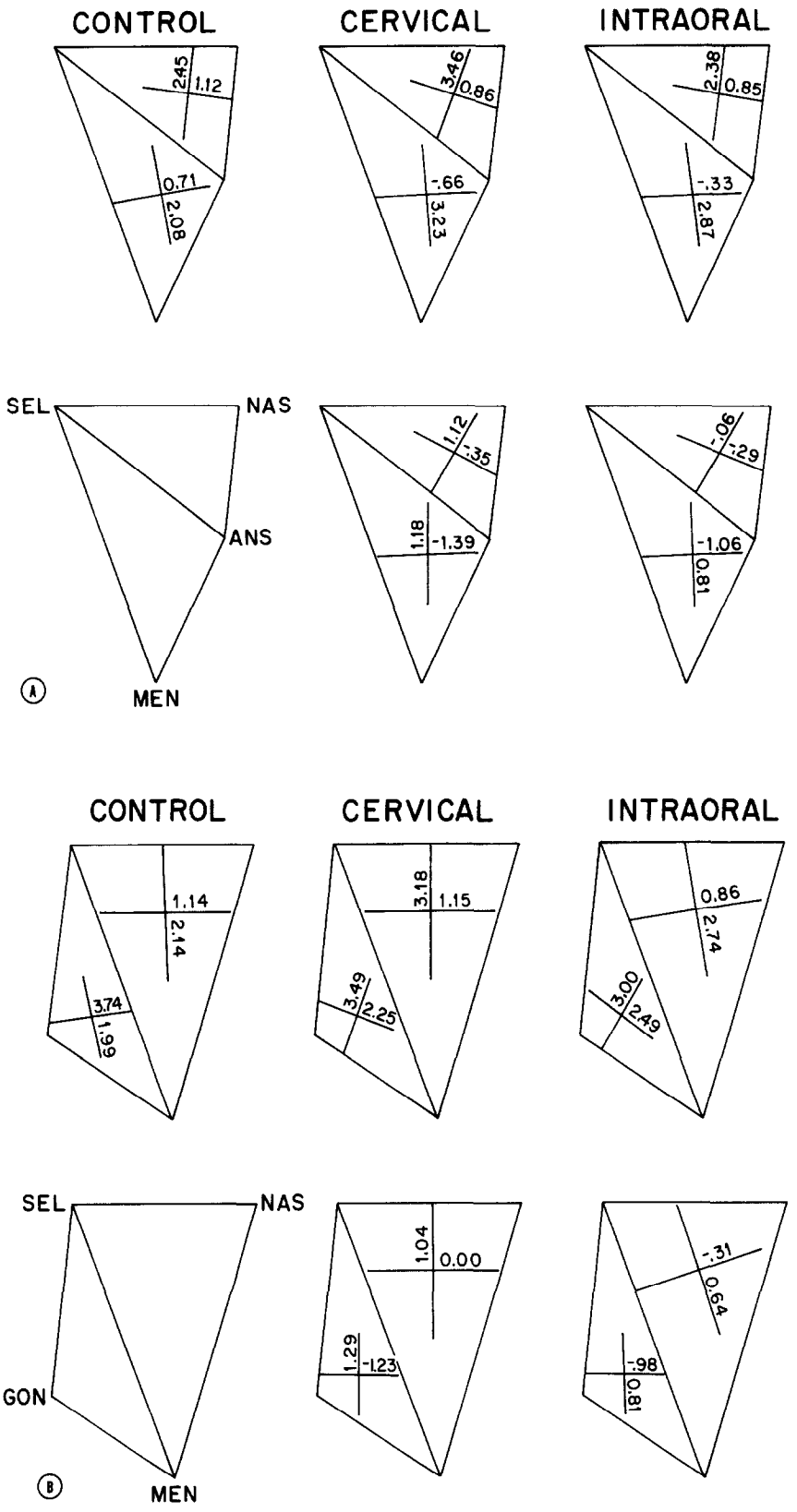

Fig. 32. Displacement of nasion. **A,** Analysis of the triangle of S-N-ANS most clearly shows the relative displacement of nasion. **B,** The large triangle S-N-M shows that cervical treatment affects net chin position perpendicular to S-N but does not affect growth along S-N.

intraoral effect. The difference between these effects may be conventionally described as extra rotation of ANS downward and backward (by about 0.7 degree per year as measured at sella) by the cervical treatment. The divergence of treatment effects at nasion may also be noted in the summary triangle S-M-N, the biorthogonal analysis of which, ignoring ANS, is shown in Fig. 32, *B*. Normal growth moves menton vertically downward from the midpoint of sella-nasion at 2.14 percent per year; cervical treatment adds precisely 1 percent per year to this rate without altering growth in the perpendicular direction, along S-N.

I do not draw any conclusions from this analysis regarding the relative merits of the treatments studied here. My purpose is only to demonstrate how the biorthogonal method, unlike the motley of predetermined distances, ratios, and angles of any "analysis," leads the investigator into straightforward and consistent summaries of the complex of adjustments and adaptations which we mean by the term "treatment effect."

CONCLUDING REMARKS

Under this heading I speak to two concerns relevant to most morphometric methods.

Assumptions of the method

The expression of displacements among landmarks by use of the tensors diagrammed here is meaningful only to the extent that the transformation may be modeled, after D'Arcy Thompson, as a smooth deformation. There should be no tearing of the picture plane, so that points previously adjacent are now widely separated—no slip of one structure relative to another, passage of points from interior to exterior of closed curves, or discontinuous opening of an angle. There should be little motion of one part over another by projection from other planes, or drift of one structure through another (as of teeth through the alveolar process); there can be no creation of new "coordinate mesh," no tissue not smoothly accounted for in earlier triangulations. And, of course, one must determine landmarks with the utmost precision, especially between films for the same subject.

There is, in addition, the postulate of *homogeneity within triangles*, without which we may not summarize deformation over a whole region by a single tensor locatable everywhere. If lines straight in one form become curved in another, or if change is not linear along homologous segments, one must determine additional landmarks which break up the curving edge into more closely spaced chords. When strictly homologous landmarks are available inside the triangles of an analysis, one might investigate this postulate of homogeneity directly by triangulating more finely.

Further developments

My group at the University of Michigan is proceeding on several projects at once. (1) The machinery of this essay yields average deformations over populations. For the technique to be of use in prediction, quantitative correlation of growth with form should be invoked to adjust the mean deformation. (2) Conventions are lacking for relating the tensor description of shape change to conclusions drawn from implant studies; these, although very precise, do not relate points homologously between individuals or even between observations on the same individual. (3) We need an atlas of conventional change patterns for quadrilaterals (triangles taken two at a time) to supplement the roster of simple standard forms in Section III. (4) With the advent of three-dimensional cephalometry via photogrammetric and computer-tomographic techniques, we need to extend all these analyses from two dimensions to three. Several researchers now explore protocols for collecting such data; their analysis will require new conventions for triangulation, quantification, and display.

The current conventions of cephalometric analysis would have us throw away nearly all the information contained in the comparison of cephalograms. If these images are to help our understanding of biologic processes, we need to begin with a measurement method explicitly suited to the comparative questions being asked. I submit the biorthogonal method set forth in this essay as the first fundamental tool appropriate to the new methodology.

I wish to acknowledge the support of N.I.D.R. grants DE-03610 to R. E. Moyers and DE-05410 to F. L. Bookstein in the course of researches reported here.

Appendix

BIORTHOGONAL ANALYSIS BY RULER AND PROTRACTOR

Given six points A, B, C, A′, B′, and C′ to find the biorthogonal directions for the distortion carrying the triangle ABC to the triangle A′B′C′ (Fig. A1, *a*):

Step 1 (Fig. A1, *b*). Choose any two vertices, here A and B. Register the triangles at $A = A'$ and orient along AB.

Step 2 (Fig. A1, *c*). Draw the line L_1 parallel to $C'B'$ through B, and construct C'', its point of intersection with AC'.

Step 3 (Fig. A1, *d*). Construct F, the midpoint of segment CC'', and draw the line L_2 through A and F.

Step 4 (Fig. A1, *e*). Draw L_3, the perpendicular to CC'' through B, and produce it until it intersects L_2 at D.

Step 5 (Fig. A1, *f*). Draw L_4 through D perpendicular to L_3 (that is, parallel to CC''), and let it intersect AC at E.

Step 6 (Fig. A1, *g*). The biorthogonal directions we seek

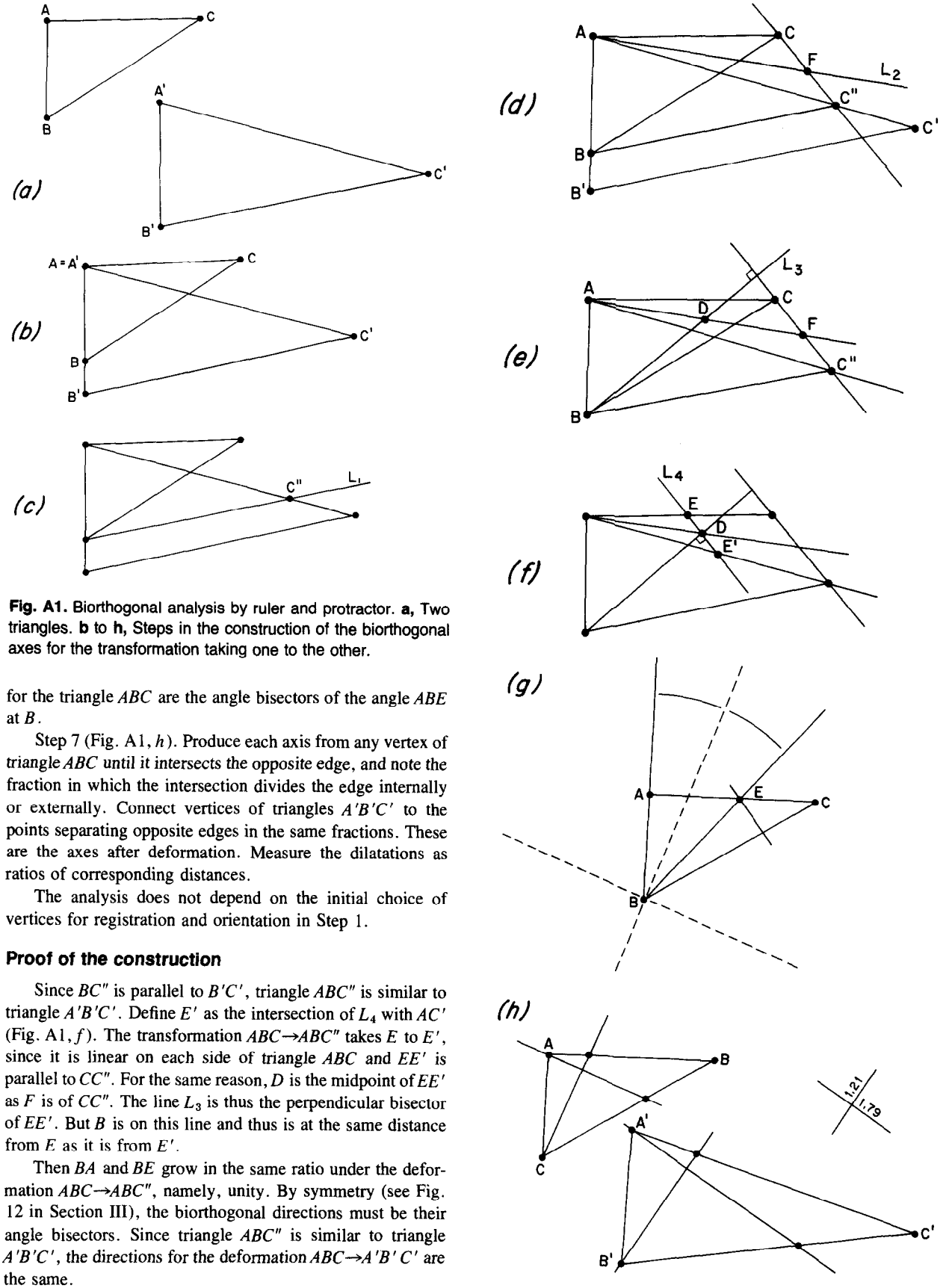

Fig. A1. Biorthogonal analysis by ruler and protractor. **a,** Two triangles. **b** to **h,** Steps in the construction of the biorthogonal axes for the transformation taking one to the other.

for the triangle ABC are the angle bisectors of the angle ABE at B.

Step 7 (Fig. A1, *h*). Produce each axis from any vertex of triangle ABC until it intersects the opposite edge, and note the fraction in which the intersection divides the edge internally or externally. Connect vertices of triangles $A'B'C'$ to the points separating opposite edges in the same fractions. These are the axes after deformation. Measure the dilatations as ratios of corresponding distances.

The analysis does not depend on the initial choice of vertices for registration and orientation in Step 1.

Proof of the construction

Since BC'' is parallel to $B'C'$, triangle ABC'' is similar to triangle $A'B'C'$. Define E' as the intersection of L_4 with AC' (Fig. A1, *f*). The transformation $ABC \rightarrow ABC''$ takes E to E', since it is linear on each side of triangle ABC and EE' is parallel to CC''. For the same reason, D is the midpoint of EE' as F is of CC''. The line L_3 is thus the perpendicular bisector of EE'. But B is on this line and thus is at the same distance from E as it is from E'.

Then BA and BE grow in the same ratio under the deformation $ABC \rightarrow ABC''$, namely, unity. By symmetry (see Fig. 12 in Section III), the biorthogonal directions must be their angle bisectors. Since triangle ABC'' is similar to triangle $A'B'C'$, the directions for the deformation $ABC \rightarrow A'B'C'$ are the same.

In the example of Fig. A1, point E lies properly between

Fig. A1 Cont'd. (Legend in preceding column.)

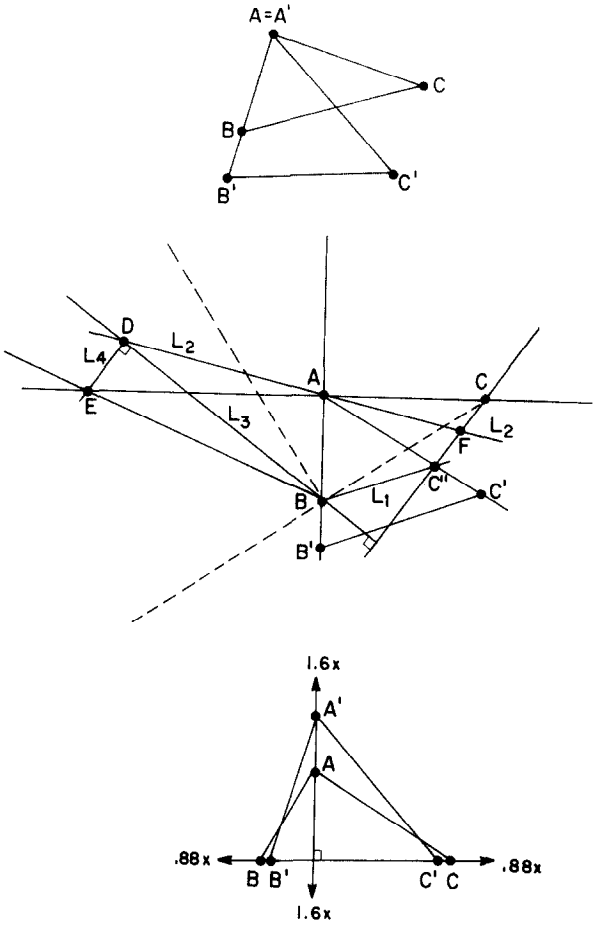

Fig. A2. A second example, in which point *E* lies outside the segment *AC*.

A and *C*. In the next example (Fig. A2), *E* is outside the segment *AC*. It happens here that the direction of least dilatation is very nearly along side *BC* of the original triangle.

For small changes of shape, with *C″* very near *C* after scaling, point *F* is nearly on top of *C* and line L_2 lies very close to line *AC*. Then points *D* and *E* coalesce as well, so that the principal axes become the bisectors at *B* of the normal from *B* to *CC″*. These bisectors, however, are at exactly 45 degrees to the bisectors of the more obvious angle between *BA* and *CC″*. There results the quick approximate construction of Fig. A3, requiring only a ruler. For instance, if after scaling to constant *AB* the point *C* appears to be moving parallel to *AB*, then the principal directions are at ±45 degrees to *AB*, as in Fig. 14, left.

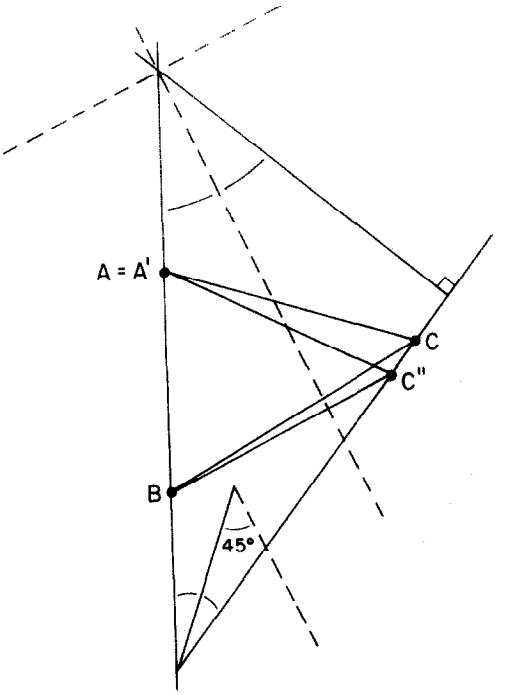

Fig. A3. The quick construction of approximate axes, appropriate when *C″* is very near to *C*.

REFERENCES

1. Baumrind, S., Korn, E. L., Molthen, R., and West, E. E.: Changes in mandibular dimensions associated with the use of force to retract the maxilla, AM. J. ORTHOD. **79:** 17, 1981.
2. Baumrind, S., and Miller, D. M.: Computer-aided head film analysis: The University of California San Francisco method, AM. J. ORTHOD. **78:** 41, 1980.
3. Baumrind, S., Molthen, R., West, E. E., and Miller, D. M.: Mandibular plane changes during maxillary retraction. Part 1. AM. J. ORTHOD. **74:**32, 1978. Part 2. AM. J. ORTHOD. **74:**603, 1978. Addenda. AM. J. ORTHOD. **75:**86, 1979.
4. Bookstein, F. L.: Looking at mandibular growth: Some new geometrical methods, pp. 83-103. *In* Carlson, D. S. (editor): Craniofacial biology, Monograph No. 10, Craniofacial Growth Series, Ann Arbor, 1981, Center for Human Growth and Development, The University of Michigan.
5. Bookstein, F. L.: The measurement of biological shape and shape change, Lecture notes in biomathematics, v. 24, Berlin, 1978, Springer-Verlag.
6. Moyers, R. E., and Bookstein, F. L.: The inappropriateness of conventional cephalometrics, AM. J. ORTHOD. **75:** 599, 1979.
7. Lanczos, C. E.: Space through the ages, New York, 1970, Academic Press, Inc.